# Mouse intact cardiac myocyte mechanics: cross-bridge and titin-based stress in unactivated cells

Nicholas M.P. King,[1,2] Methajit Methawasin,[1] Joshua Nedrud,[1] Nicholas Harrell,[1] Charles S. Chung,[1] Michiel Helmes,[3] and Henk Granzier[1]

[1]Department of Physiology and Molecular Cardiovascular Research Program and [2]Department of Cell Biology and Anatomy, University of Arizona, Tucson, AZ 85724
[3]University of Oxford, Oxford OX1 2JD, England, UK

A carbon fiber–based cell attachment and force measurement system was used to measure the diastolic stress–sarcomere length (SL) relation of mouse intact cardiomyocytes, before and after the addition of actomyosin inhibitors (2,3-butanedione monoxime [BDM] or blebbistatin). Stress was measured during the diastolic interval of twitching myocytes that were stretched at 100% base length/second. Diastolic stress increased close to linear from 0 at SL 1.85 µm to 4.2 mN/mm$^2$ at SL 2.1 µm. The actomyosin inhibitors BDM and blebbistatin significantly lowered diastolic stress by ~1.5 mN/mm$^2$ (at SL 2.1 µm, ~30% of total), suggesting that during diastole actomyosin interaction is not fully switched off. To test this further, calcium sensitivity of skinned myocytes was studied under conditions that simulate diastole: 37°C, presence of Dextran T500 to compress the myofilament lattice to the physiological level, and [Ca$^{2+}$] from below to above 100 nM. Mean active stress was significantly increased at [Ca$^{2+}$] > 55 nM (pCa 7.25) and was ~0.7 mN/mm$^2$ at 100 nM [Ca$^{2+}$] (pCa 7.0) and ~1.3 mN/mm$^2$ at 175 nM Ca$^{2+}$ (pCa 6.75). Inhibiting active stress in intact cells attached to carbon fibers at their resting SL and stretching the cells while first measuring restoring stress (pushing outward) and then passive stress (pulling inward) made it possible to determine the passive cell's mechanical slack SL as ~1.95 µm and the restoring stiffness and passive stiffness of the cells around the slack SL each as ~17 mN/mm$^2$/µm/SL. Comparison between the results of intact and skinned cells shows that titin is the main contributor to restoring stress and passive stress of intact cells, but that under physiological conditions, calcium sensitivity is sufficiently high for actomyosin interaction to contribute to diastolic stress. These findings are relevant for understanding diastolic function and for future studies of diastolic heart failure.

## INTRODUCTION

Systolic properties have been well studied from the whole heart down to the single myosin molecule. In contrast, diastolic properties of the heart, which underlie the filling characteristics of the cardiac cycle, are less well understood. It is important to thoroughly understand the various mechanisms that underlie diastolic stress, considering that increased diastolic stress is a primary defect in diastolic heart failure (DHF; also known as heart failure with normal ejection fraction), and that DHF is rapidly increasing in prevalence without effective therapies (Zile and Brutsaert, 2002a,b; Kass et al., 2004; Bronzwaer and Paulus, 2005; Owan et al., 2006). One particular portion of diastole that lacks a clear mechanism is diastolic suction. When active contraction of a ventricle ends, the ventricle rapidly expands and sucks blood (diastolic suction) into the ventricle, before contraction of the atria pumps blood into the ventricle. The extent of early filling of the heart is an important indicator of diastolic function (Zile and Brutsaert, 2002b;

Nishimura and Jaber, 2007). One proposed ventricular suction model involves twisting of the heart during contraction that builds up potential energy; this is then released as diastolic suction at the end of systole (Bell et al., 1998). A cellular analogue of diastolic suction is the restoring stress that isolated cardiac myocytes generate when they actively shorten to below their slack length (length with zero passive stress) and that pushes outward on the cell, so that when activation ceases, the cell's slack length is restored. (Note that the stress that develops when the passive cell is stretched above the slack length is operationally defined as passive stress, and the stress induced by shortening below slack is defined as restoring stress.)

An important candidate to generate restoring stress in cells is the protein titin, which spans half of the smallest contractile unit of striated muscle, the sarcomere, with a molecular spring region in the I-band region of the sarcomere that develops force when extended (Labeit and Kolmerer, 1995; Krüger and Linke, 2009;

---

N.M.P. King and M. Methawasin contributed equally to this paper.
Correspondence to Henk Granzier: granzier@email.arizona.edu

Abbreviations used in this paper: BDM, 2,3-butanedione monoxime; DHF, diastolic heart failure; FSM, Frank–Starling mechanism; SL, sarcomere length.

LeWinter and Granzier, 2010). Previous studies have resulted in a model where titin's molecular spring functions bi-directionally: in sarcomeres extended above slack, the spring is stretched away from the Z-disk, resulting in passive force; in sarcomeres shortened to below slack, the spring is extended in the opposite direction, developing restoring force (for details see Helmes et al., 1996, 2003; Trombitás and Granzier, 1997; Trombitás et al., 2001; Preetha et al., 2005).

Previous work has all been done on cardiac myocytes whose membrane was chemically permeabilized (skinned), which has as a drawback swelling of the myofilament lattice that occurs upon skinning and the loss of soluble proteins; the goal of the present work was to study intact cells, leaving in place cellular characteristics lost upon demembranization—soluble proteins, signaling pathways, cytoskeletal proteins, and their networks. Technical limitations have previously hampered work on intact cardiomyocytes (Brady, 1991), but these have now been overcome through pioneering work from various groups (Le Guennec et al., 1990; Yasuda et al., 2001; Iribe et al., 2007), which resulted in the recent development of a carbon fiber system for cell attachment and force measurement. We used this approach and characterized diastolic properties of intact cells before and after the addition of cross-bridge inhibitors (2,3-butanedione monoxime [BDM] and blebbistatin). Results were compared with those of previous studies on skinned myocytes (Helmes et al., 1996, 2003; Preetha et al., 2005) and intact trabeculae (Backx, 1989). We also studied actomyosin interaction in unactivated intact cells and in skinned cells at diastolic calcium levels. The findings of these studies establish the passive properties of mouse intact cardiac myocytes, including their restoring stress–SL relation, and provide evidence for the existence of actomyosin interaction under physiological conditions at diastolic calcium levels.

## MATERIALS AND METHODS

### Cardiomyocyte isolation
Approximately 4-mo-old male C57BL/6 mice were used. Experiments were conducted in accordance with the Guide for the Care and Use of Laboratory Animals, and all protocols were approved by University of Arizona's Institutional Animal Care and Use Committee. Cells were isolated as described previously (O'Connell et al., 2007). In brief, after cervical dislocation and while under anesthesia via isoflurane inhalation, the heart was dissected and cannulated via the aorta. The heart was perfused for 4 min with perfusion buffer (in mM: 113 NaCl, 4.7 KCl, 0.6 $Na_2HPO_4$, 1.2 $MgSO_4$, 12 $NaHCO_3$, 10 $KHCO_3$, 10 HEPES, and 30 taurine, pH 7.4), followed by perfusion with digestion buffer (perfusion buffer plus 0.45 mg/ml collagenase II [240 U/mg; Worthington Biochemical Corporation], 0.13 mg/ml trypsin, and 25 µM $CaCl_2$) for 8–10 min. When the heart was flaccid, digestion was halted and the heart was placed in myocyte stopping buffer 1 (perfusion buffer plus 0.04 ml bovine calf serum [BCS]/ml buffer and 5 µM $CaCl_2$). The left ventricle was cut into small pieces, and the rest of the heart was discarded. The small pieces of left ventricle were then triturated several times with a transfer pipette and then filtered through a 300-µm nylon mesh filter. After this, the cells were gravity pelleted and the supernatant was discarded. Next, 10 ml of myocyte stopping buffer 2 was added (perfusion buffer plus 0.05 ml BCS/ml buffer and 12.5 µM $CaCl_2$), and $Ca^{2+}$ was reintroduced to a final concentration of 1.8 mM. Cell pellets were solubilized and electrophoresed (Warren et al., 2003; Lahmers et al., 2004) to determine titin content.

### Intact cardiomyocyte mechanics
An inverted microscope (IX-70; Olympus) was used with a modified chamber to mount our mechanics apparatus. The chamber has platinum electrodes to electrically stimulate cells and a perfusion line with heater control and suction out to maintain a flow rate of ~1 ml/min. Sarcomere length (SL) and cell edge displacement were measured with a 1,000-Hz MyocamS (IonOptix) attached to a computer. Data were collected using an IonOptix FSI A/D board and IonWizard software with SarcLen and SoftEdge modules to determine SL and carbon fiber displacement, plus a custom module for determining real-time force. The sampling frequency of the system was sufficient to measure force (1,000 Hz) and SL (250 Hz) simultaneously. Carbon fibers were used (10 µm cfs; b-1; TMIL Ltd.) that were mounted in custom-pulled and angled glass pipettes (0.7–1.2 mm of carbon fibers protruding from pipette tip), and their stiffness was determined by cross-calibrating with a force transducer (model 406A; Aurora Scientific). The carbon fiber was displaced by the force transducer to ~10 different lengths twice, and then force versus displacement was plotted to determine the slope (stiffness) of each carbon fiber previous to use. Stiffness ranged from 0.06 to 0.36 µN/µm, giving rise to a force resolution of 0.006–0.036 µN.

Cells were attached as described previously (Iribe et al., 2007). In brief, after adding cells to the chamber, they were allowed to settle on a poly-HEMA (Sigma-Aldrich)–coated coverslip. A rod-shaped cell was selected, and the carbon fibers were carefully lowered onto opposite ends of the cell. Perfusion was started at this point with 1.0 mM $Ca^{2+}$ tyrode (10 mM HEPES, 11.1 mM glucose, 5 mM Na pyruvate, 1.8 mM $CaCl_2$, and 2.5 U/liter insulin) at 37.5°C. The cell was slightly pressed between the coverslip and the carbon fibers, and electrical twitch stimulating was begun at 4 Hz for 5 min. After 5 min, the cells were lifted off the coverslip. Once attached, the cells were electrically stimulated at 0.5 Hz. A triangular stretch–release protocol was used to elucidate the force–SL relation, and the carbon fiber movement explained earlier was controlled via custom LabVIEW software. Cells were stretched at 100% base length/second to varying amplitudes. All forces were normalized to stresses (force/unit undeformed cross-sectional area [CSA]), with the CSA determined by assuming that the cross section is an ellipse with CSA = $\pi*1/2$width$*1/2$thickness. This CSA was compared with our previous method of directly measuring the CSA, in which we lift one side of the cell vertically and record the image of the cross section and directly measure CSA (see Granzier and Irving, 1995). The measured values were not significantly different from those calculated.

### Actomyosin cross-bridge inhibition
To inhibit actomyosin cross-bridge interaction, cells were perfused with 30 mM BDM (Backx et al., 1994) or 22.5 µM blebbistatin (Sigma-Aldrich) (Farman et al., 2008). Cells perfused with blebbistatin had a red filter over the light source to prevent breakdown of blebbistatin. It took ~100 s for complete cessation of contractility after the cells were perfused with inhibitor.

### Skinned cell mechanics
Mouse cells, isolated as explained above, were skinned for 7 min in relaxing solution (in mM: 40 BES, 10 EGTA, 6.56 $MgCl_2$, 5.88

Na-ATP, 1.0 DTT, 46.35 K-propionate, 15 creatine phosphate, 0.1 leupeptin, 0.1 E64, and 0.2 PMSF, pH 7.0) with 0.3% Triton X-100 (ultrapure; Thermo Fisher Scientific). Cells were washed extensively with relaxing solution and stored on ice. Cells were then added to a temperature-controlled chamber that was mounted to the stage of an inverted microscope. Cells were glued (silicone rubber sealant) at one end to a force transducer (model 406A; Aurora Scientific) and at the other end to a high speed length controller (model 308B; Aurora Scientific). Measured forces were converted to stress as described previously (Granzier and Irving, 1995). We compared the obtained stresses of skinned cells to those of intact cell. Because it is known that skinning results in myofilament lattice expansion, we performed experiments in which we added to all solutions 4.5% of the osmotic agent Dextran T500, a level which compresses the lattice back to the in vivo spacing (Irving et al., 2000; Farman et al., 2006). Furthermore, to ensure that cells were completely passive, we added 22.5 µM blebbistatin. SL was measured on-line using a system identical to the one described above for the intact cell work. Cells were stretched at a speed of 100% base length/second to a SL of 2.2 µm, followed by a 20-s hold and then a release back to the original length. Stretch–hold–release protocols were repeated after a 7-min rest at slack length. Experiments were performed at 37°C (note that the relaxing solution pH was adjusted to 7.0 at the temperature used). Temperature was measured with a thermistor probe, positioned in the chamber near the cell, and was within 0.5 deg of the target temperature during experiments. Cells were characterized before and after the addition of blebbistatin (see above for details). In experiments in which the effect of calcium on diastolic stress of skinned cells was studied, free calcium concentrations were calculated according to Fabiato and Fabiato (1979), with parameters adjusted for the experimental temperatures used (37°C).

### Statistics

Data were analyzed with a Student's $t$ test or, where appropriate, with ANOVA. A p-value of $<0.05$ was considered significant. Curves were fit using KaleidaGraph 4.0 (Synergy Software). All values are the mean ± SE unless otherwise noted.

## RESULTS

### Intact cardiomyocyte diastolic stress

An example of a mouse cardiac myocyte that was twitch activated and stretched via carbon fibers with a ramp stretch and release protocol imposed during a prolonged diastolic interval is shown in Fig. 1 A. As is seen in the expanded example traces of Fig. 1 B, cardiomyocytes respond to stretch by exhibiting a characteristic
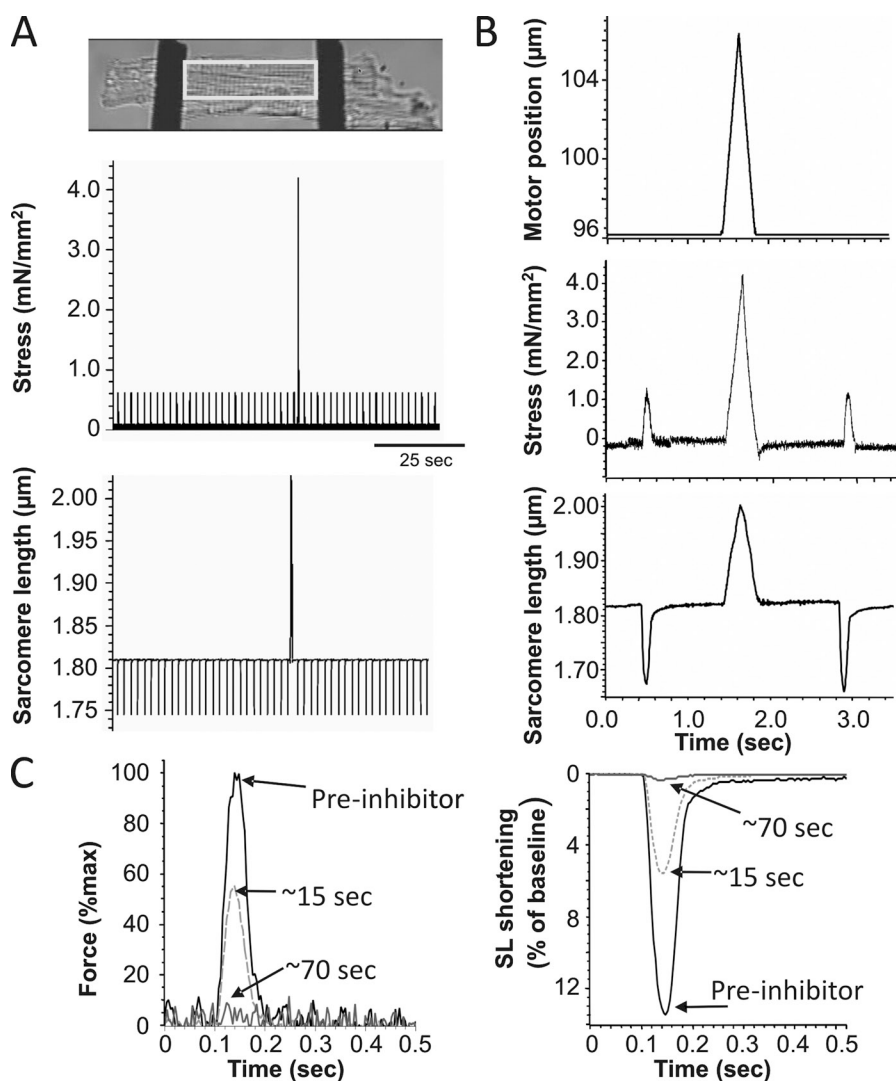


Figure 1. Experimental approach. (A; top) A representative intact cardiomyocyte attached to carbon fibers (black bars on either side of cell). The outlined area is a typical region of measurement for SL. (Middle) Carbon fiber displacement was tracked and converted to cell stress (see Materials and methods). (Bottom) SL traces. (B) Explanation of single triangle stretch and release protocol with an electrically stimulated twitch on either side. The top panel is the motor movement applied to the cell over time. The middle panel shows the expanded ramp–release stress trace, and the bottom panel is the SL trace. (Note that the cells were normally twitching at 0.5 Hz but that the diastolic interval was prolonged when a stretch–release was imposed.) (C) Twitch force (left) and SL shortening (right) for a cell before (pre-inhibitor) the cross-bridge inhibitor, shortly after the cross-bridge inhibitor (BDM) begins acting on the cell (~15 s), and after the full effect of the cross-bridge inhibitor (~70 s).

force response while the subsequent release returns the cell to the starting SL. Stretching the cell across the physiological SL range elicited a diastolic stress response that was repeatable within each cell. Thus, the system is robust and makes it possible to determine the diastolic stress–SL relation of intact cardiomyocytes. To explore the possibility that diastolic stress of intact cardiomyocytes is in part a result of actomyosin interaction, diastolic stress was also measured in the presence of the actomyosin inhibitor blebbistatin or BDM (selected because of their different mechanisms of inhibition; blebbistatin binds to a hydrophobic pocket at the apex of the 50-kD cleft of myosin and keeps the cleft partially open, trapping myosin in a state with low actin affinity [Kovács et al., 2004], and BDM inhibits the rate of phosphate release, stabilizing the M-ADP-Pi state of the ATPase cycle [Herrmann et al., 1992]). With either inhibitor, a reduction in twitch force and SL shortening occurred within seconds, until both were indistinguishable from system noise (typically within ∼100 s; see Fig. 1 C for examples).

Although diastolic stress–SL results from individual cells were slightly curvilinear, the average of all 19 cells that were studied increased close to linear with changes in SL (Fig. 2, open circles). When actomyosin-inhibited cells were stretched, passive stress was reduced relative to the relation before inhibition, with similar result for BDM and blebbistatin (Fig. 2, squares and diamonds, respectively). The stress reduction in the presence of the inhibitors suggests that the diastolic stress of intact mouse cells has an actomyosin contribution. This conclusion is supported by measurements of resting SL of unattached intact cells. In the absence of inhibitor the resting SL was ∼1.84 µm, and in the presence of inhibitor it increased to ∼1.93 µm (Tables I and II). The SL dependence of active stress contribution to diastolic stress is shown in Fig. 3 A. The average reduction at all SLs is ∼1.5 mN/mm$^2$, with a trend toward lower values at longer SLs (see also Discussion)

and no significant difference between the results with the two inhibitors.

Because we wished to compare the diastolic stress of intact cells to that of skinned cells, we first studied whether mouse skinned myocytes in relaxing solution are fully passive (at 37°C). This was addressed by studying skinned cells that were glued at one end to the servomotor and lifted away from the coverslip bottom of the chamber. Thus, the cells were only attached at one end and were free to change length in response to the addition of blebbistatin. It was found that the resting SL was slightly but significantly increased by blebbistatin, from 1.85 ± 0.02 to 1.89 ± 0.02 (paired $t$ test p-value of 0.004). When these experiments were repeated at lower temperatures, it was found that blebbistatin had no effect on either stress or slack SL at 14 or 24°C (not depicted). Thus, skinned cells in relaxing solution are fully passive at 14 and 24°C, but at physiological temperatures, they develop a low level of active stress. We then measured the passive stress of skinned myocytes, using experimental conditions that were the same as those for intact cells (37°C; stretch speed 100%/s; 4.5% Dextran to reduce the myofilament spacing to that of intact cells [see also below]; presence of 22 µM blebbistatin). The obtained passive stress–SL relation was similar to that of intact cells in the presence of inhibitors (Fig. 2, filled circles).

Our results suggest that high diastolic stresses of intact cells are due in part to calcium-induced actomyosin interaction. To test this further, we performed a series of experiments in which we established the effect of low levels of calcium on the stress of skinned myocytes at 37°C. We did experiments in which we added 4.5% of the osmotic agent Dextran T500, a level that compresses the lattice back to the in vivo spacing (Irving et al., 2000; Farman et al., 2006), and compared results to those in the absence of Dextran. Results show that in the absence of Dextran, a significant level of active stress is generated at [Ca$^{2+}$] > 175 nM; in the presence of Dextran,
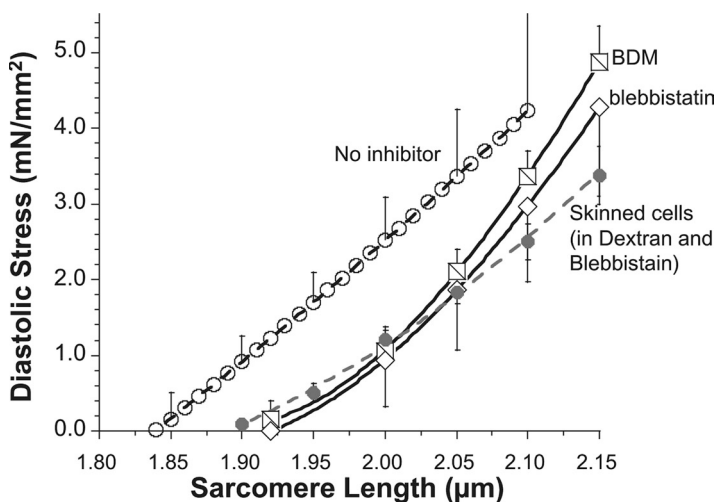


**Figure 2.** Diastolic stress–SL relationship of intact and skinned cardiomyocytes. Mean diastolic stress–SL relationship of mouse intact cardiomyocytes before inhibitor (open circles) and after actomyosin inhibition with BDM (squares) or blebbistatin (diamonds). Results are also shown for mouse skinned myocytes studied in 4.5% Dextran and in the presence of blebbistatin (gray-filled circles). For clarity, not every SE is shown. Force measured during a stretch with speed 100% base length/second; temperature, 37°C.

### TABLE I
*Unloaded intact cardiac myocytes*

| Treatment | SLr of intact cardiac myocytes (µm) |
|---|---|
| Control | $1.84 \pm 0.003$ ($n = 268$) |
| 30 mM BDM | $1.90 \pm 0.003$ ($n = 101$)[a] |
| 22.5 µm blebbistatin | $1.93 \pm 0.005$ ($n = 172$)[a] |

Resting SL ($SL_r$) measurements of intact unloaded cardiomyocytes. The resting SL (mean ± SE) of cardiocytes was measured for unloaded cells with no inhibitor (control), treated with BDM, or treated with blebbistatin. See text for details.

[a]ctrl versus treatment, P < 0.001.

### TABLE II
*Loaded intact cardiac myocytes*

| Treatment | Zero stress SL (µm) |
|---|---|
| 30 mM BDM | $1.95 \pm 0.02$ ($n = 19$) |
| 22.5 µm blebbistatin | $1.97 \pm 0.04$ ($n = 16$) |

Slack SL (length with zero force) in loaded cells. The mechanically determined slack SL is not significantly different between the two inhibitors (P = 0.50). See text for details.

cells are more sensitive and active stress is produced at $[Ca^{2+}] > 55$ nM (Fig. 3 B).

### Restoring stress

When intact cells attached to carbon fibers and held at their original resting length were exposed to BDM or blebbistatin, diastolic stress gradually decreased below
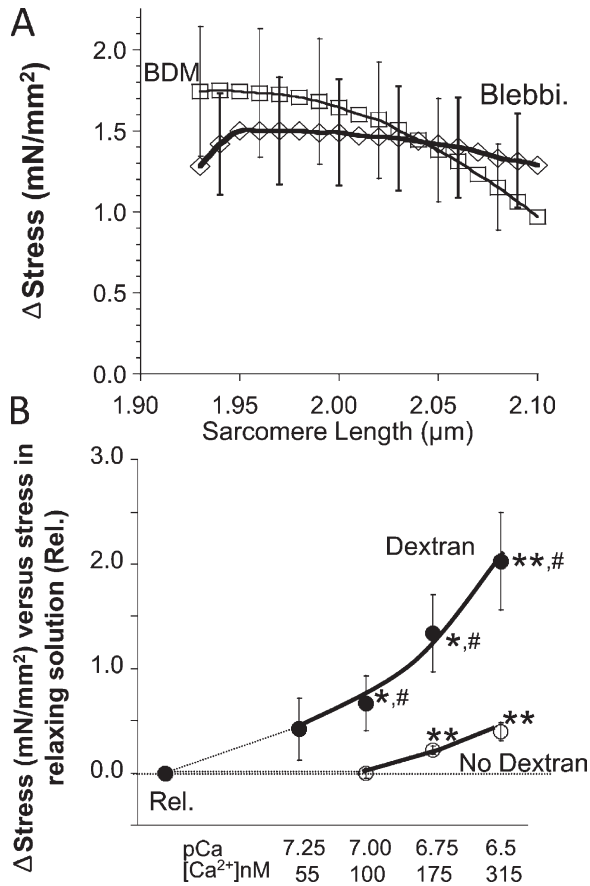


**Figure 3.** Effect of actomyosin inhibition on diastolic stress of intact cells and effect of low levels of calcium on stress of skinned cells. (A) Diastolic stress reduction of intact cells in blebbistatin and BDM (for clarity, not every SD is shown). (B) Effect of calcium on diastolic stress of skinned myocytes at 37°C in the absence (open circles) and presence of 4.5% Dextran (filled circles). *, paired *t* test of Δstress versus stress in relaxing solution; #, unpaired *t* test of Δstress in Dextran versus no Dextran.

zero and SL increased above its starting value (Fig. 4). Both stress and SL reached a steady state ∼100 s after the addition of inhibitors (as shown by slope analysis of SL and stress traces). A likely interpretation for these findings is that the quiescent cell before the addition of inhibitor developed active stress that shortened the cell until active stress was balanced by the restoring stress that pushes outward on the sarcomeres. When active stress is abolished in cells attached to carbon fibers, the restoring stress will push outward on the sarcomeres and force becomes negative until a new steady state is reached when the outwardly pushing restoring force and inwardly directed force of the carbon fibers are balanced (schematically indicated in Fig. 5 A, inset). The newly established steady state will have an increased SL and a stress that is negative. This negative stress will equal the restoring stress at the measured steady SL.

When cells in the presence of inhibitors were stretched, restoring stress became less negative, reached zero, and then became positive. An example of a stretch curve is shown in Fig. 5 A, and mean results from 19 (BDM) and 16 (blebbistatin) cells are shown in Fig. 5 B. Results with the two inhibitors were similar (P = 0.47), and both curves had a slight curvature. The stress–SL curves had a zero stress crossing of $1.95 \pm 0.02$ µm (BDM) and $1.97 \pm 0.04$ µm (blebbistatin). The slopes below and above the zero stress point represent the restoring stiffness and passive stiffness, respectively. The mean stiffness values were ∼17 mN/mm$^2$/µm/SL and were not statistically different from each other (see Fig. 5 B, inset).

### DISCUSSION

We used the recently established carbon fiber technique to study the diastolic properties of isolated mouse intact cardiac myocytes and compared the results to those of skinned cardiac myocytes, studied under identical experimental conditions. The diastolic stress of intact cells was found to significantly exceed that of skinned cells. The use of actomyosin inhibitors revealed that this difference can largely be explained by actomyosin interaction in intact cells. Studies on the calcium sensitivity of skinned cells support this conclusion. Attaching the cells to carbon fibers and then adding actomyosin inhibitors made it possible to measure the restoring stress–SL relation of intact cells. The findings of this work and their implications are discussed in detail below.
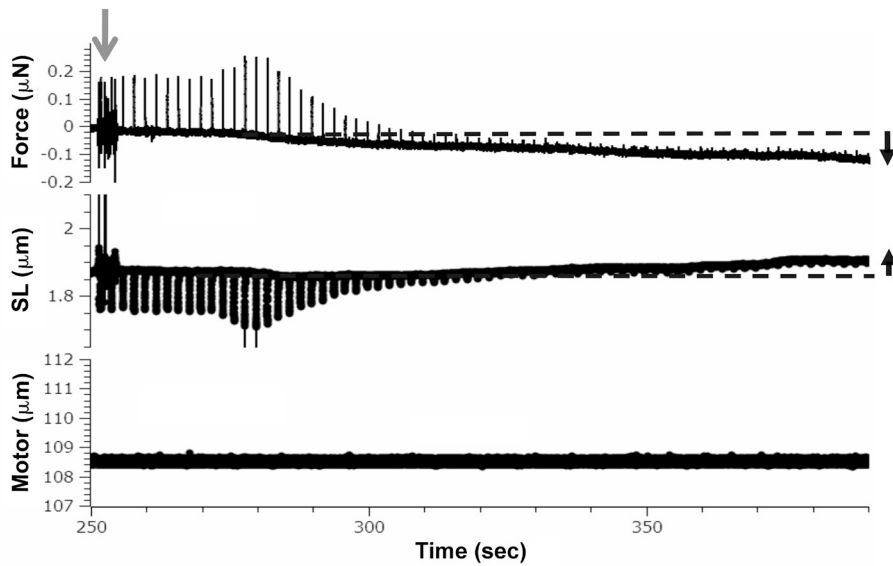
**Figure 4.** Representative force and SL traces during perfusion of blebbistatin, highlighting the presence of restoring force. Three time-matched panels of force (top), SL (middle), and motor movement (bottom) at the start of cross-bridge inhibitor perfusion (arrow). Note the decrease in diastolic force and the increase in diastolic SL over time.

### Actomyosin interaction contributes to diastolic stress of intact cells

Comparing the diastolic stress–SL relation of intact cardiocytes to that of mouse skinned cardiocytes indicates that intact cells develop much higher stresses than skinned cells (Fig. 2). A high diastolic stress level in intact cells is not unprecedented and was also reported in by Yasuda et al. (2005), who found that wild-type mouse cells develop ~1.5 mN/mm$^2$ of diastolic stress at an SL of 1.85 μm and ~4.0 mN/mm$^2$ at an SL of 2.10 μm.

Because we found that the addition of either BDM or blebbistatin significantly reduces diastolic stress (Figs. 2 and 3 A), we conclude that the high diastolic stress of intact cells results in part from actomyosin interaction. This is supported by our findings that at physiological temperature and in the presence of Dextran, skinned myocytes develop active stress at calcium levels as low as 100 nM and that the required calcium level is considerably higher in absence of Dextran. These results are consistent with previous reports that show that at
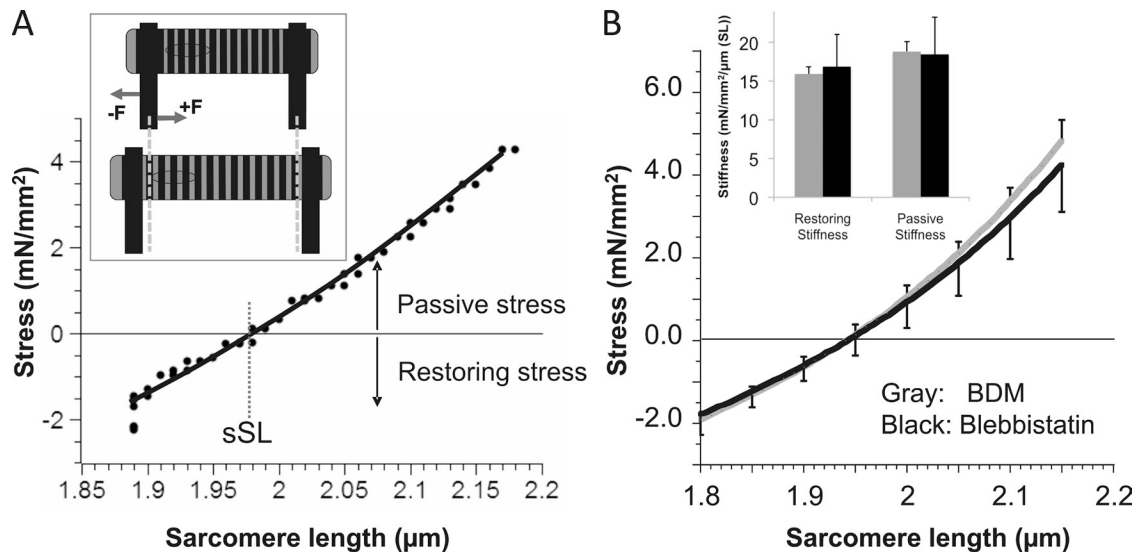


**Figure 5.** Restoring stress–SL relation. (A) The top of the schematic shows the pre-inhibition resting length of a cell with a net zero stress. The bottom of the schematic shows the cell after actomyosin inhibition. With the loss of active stress, the cell lengthens (pushing outward on the carbon fibers) until a steady state is reached, at which restoring stress is balanced by the inwardly directed stress of the carbon fibers. The main figure represents the passive stress–SL relationship for an individual cell after inhibition by blebbistatin. When the cell was stretched, restoring stress became less negative until stress was zero (slack SL, sSL ~1.97 μm), after which stress became positive. (B) Mean stress–SL relationship. Results obtained from cells inhibited with either BDM (gray; n = 19) or blebbistatin (black; n = 16). The curves are not significantly different from each other. The restoring and passive stiffness (slope of stress–SL relation) was determined 0.1 μm below and above the SL with zero stress, respectively. Results are shown in the inset (gray, BDM; black, blebbistatin). ANOVA analysis indicates that the values are not significantly different (P = 0.8).

physiological myofilament lattice spacing, calcium sensitivity is higher than in the expanded lattice of skinned muscle in relaxing solution (Farman et al., 2006) and that temperature is a positive inotrope, especially in rodents where calcium sensitivity at physiological temperature is much larger than at low temperature (Harrison and Bers, 1989, 1990).

The level of active stress of intact myocytes was relatively constant at ~1.5 mN/mm$^2$ along the measured SL range (Fig. 3 A). It is well known that because of the Frank–Starling mechanism (FSM), a given level of submaximal activating calcium results in active stress that increases with SL (Kentish et al., 1986); thus, the constant active stress that we found is unexpected. A possibility is that stretching intact cells results in a reduction of the diastolic calcium level, thereby offsetting the FSM-induced increase. However, the work by Yasuda et al. (2005) showed that diastolic calcium of mouse intact cardiac myocytes does not change when cells are stretched from an SL of 1.8 to 2.1 μm, consistent with preliminary studies performed by us (unpublished data); thus, it is unlikely that a reduction in calcium levels with stretch explains our findings. Hence, our results suggest that the low calcium level that exists in intact cardiac myocytes (estimated at ~75–150 nM; Gao et al., 1994; Stuyvers et al., 1997; Yasuda et al., 2005) does not result in a measurable Frank–Starling effect. This conclusion is consistent with the work of Adhikari et al. (2004), who conclude that the magnitude of the Frank–Starling effect is calcium dependent and peaks at ~3 μM Ca$^{2+}$ but is much reduced at low Ca$^{2+}$ levels. It is possible that at higher stimulation frequencies where diastolic calcium levels are elevated (Gao et al., 1994), higher diastolic stresses are found with a passive component (BDM/blebbistain insensitive) that is independent of pacing frequency and an active component (BDM/blebbistatin sensitive) that displays FSM behavior. Clearly, future work is needed to better understand the

effects of low levels of diastolic calcium on actomyosin interaction, including studies that determine the diastolic stress–SL relationship as a function of the extracellular calcium concentration and the effect of Ca$^{2+}$ channel blockers or Ca$^{2+}$ sensitizers. We conclude that the low level of diastolic calcium that exists in intact mouse cardiac cells under our experimental conditions does not cause a Frank–Starling effect but instead sets an SL-independent basal diastolic "tone" of the cell.

Mechanisms that underlie elevated diastolic stress in DHF are currently under intense investigation, and it is likely that changes in titin isoform expression and post-translational modification play a role (Borbély et al., 2005, 2009a,b; Hamdani et al., 2008). However, current research is largely based on studying skinned cardiac myocytes at low temperature, because the skinned myocyte is a relatively convenient preparation to use and the low experimental temperature increases the repeatability of the mechanical responses. Our findings suggest that such studies miss the actomyosin contribution to diastolic stress under physiological conditions and its possible role in elevated diastolic stress in DHF. Future studies on cellular mechanisms underlying DHF may reveal more (patho)physiological information if they are performed on both intact and skinned preparations, and at physiological temperatures.

### Restoring stress

Abolishing actomyosin interaction in intact cells that had been held at their unattached length resulted in a negative stress (i.e., a stress that pushes outward on the carbon fibers). This can be explained by the existence of active stress that shortens unattached cells to below their slack length and a restoring stress that increases with shortening amplitude; a steady-state SL is reached when the active stress equals the restoring stress. Thus, when active stress is abolished, the net stress will be negative and the cell will lengthen until a new steady state is
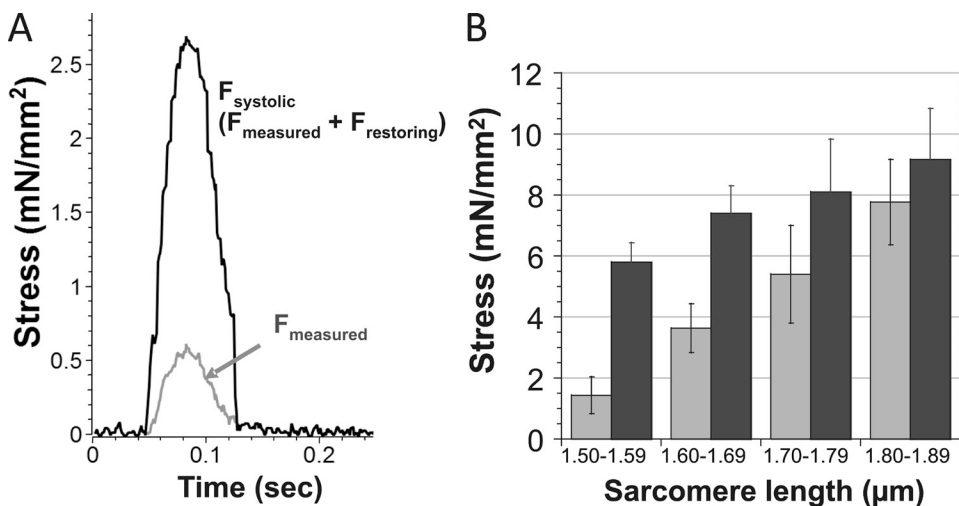


Figure 6. Twitch stress correction as a result of restoring stress in contraction below slack SL. (A) By adding the restoring stress to the measured stress (gray) for the specific SL during a twitch contraction, the true systolic stress was determined (black). (B) The measured (gray) and corrected (black) peak twitch stress binned in 0.1-μm SL intervals.

reached at which the restoring stress equals the stress exerted by the carbon fibers (Fig. 5 A, inset). Stretching the cell from this new equilibrium length results in a reduction of restoring stress until the slack length (length with zero force) is reached, with further stretch resulting in the development of passive stress. The slopes of the restoring stress–SL and passive stress–SL relations around the slack length are indistinguishable (Fig. 5 B, inset). This finding is consistent with a model previously proposed in which titin functions as a bi-directional spring that develops passive stress above the slack length and restoring stress below the slack length (Helmes et al., 1996; Preetha et al., 2005). The near–Z-disk region of titin that interacts with actin and is therefore functionally stiff underlies this bi-directionality (Trombitás and Granzier, 1997; Granzier et al., 2000; Trombitás et al., 2000). When the sarcomere shortens to below the slack length, thick filaments move into this near–Z-disk region, extending titin in a direction that is opposite of when sarcomeres are extended to above the slack length (see schematic in Fig. 7 B).

Stretching cells from a starting length with restoring stress makes it possible to mechanically determine the slack SL (i.e., the SL at which force is zero). The obtained SL was 1.95 µm (BDM) and 1.97 µm (blebbistatin). This value is much longer than the SL of unloaded intact cells measured by us (1.84 µm; Tables I and II) as well as reported by others, with published values typically between 1.7 and 1.8 µm (Nash et al., 1979; Wussling et al., 1987; Niggli, 1988; Roos and Brady, 1989; Le Guennec et al., 1990; Bluhm et al., 1995; Neagoe et al., 2003; Lorenzen-Schmidt et al., 2005; Ter Keurs et al., 2008; Flagg et al., 2009; Bub et al., 2010). An obvious explanation for this discrepancy is that unloaded intact cells develop active stress that shortens cells to below their slack SL, consistent with our finding that the SL of unloaded intact cells is increased when actomyosin inhibitors are added (Tables I and II). In summary, our work establishes that the slack SL of isolated intact mouse cardiac myocytes at physiological temperatures can only be obtained in the presence of actomyosin inhibitors and that the mechanically determined slack SL value is ∼1.95 µm.

The peak active stress levels that were produced by the twitch contractions were relatively low. For example, at a systolic SL of 1.6–1.7 µm, the mean active stress was ∼4 mN/mm$^2$. Low values have also been reported by others (Le Guennec et al., 1990; Yasuda et al., 2001; Iribe et al., 2007). It is important to note that the presence of restoring stress will mask the real active stress levels, and the lower than expected systolic stress may be explained by a sum of the forces involved during a twitch contraction: the positive systolic (active) component and the negative restoring stress component. The measured restoring stress–SL relation allows us to add the restoring stress to the measured stress and obtain the actual systolic stress (Fig. 6 B). We can compare obtained values to the reported twitch stresses of mouse trabeculae, with measurements reported by Gao et al. (1998) and Stuyvers et al. (2002) with a stimulation frequency of 0.5 Hz (the same as frequency as our study). Gao et al. (1998) reported a twitch stress of ∼7.5 mN/mm$^2$, and Stuyvers et al. (2002) reported ∼12.5 mN/mm$^2$. Both of these studies were performed at a diastolic SL of ∼2.0–2.1 µm, and with the given level of internal shortening (Fig. 2 B; Stuyvers et al., 2002), the systolic SL was likely ∼1.8–1.9 µm. At this systolic SL range, we measured active stress levels of ∼8 mN/mm$^2$ (Fig. 6 B). Thus, the active stress levels that we measured, accounting for the restoring stress, are similar to those reported for trabeculae. We also conclude that at short SL, the level of restoring stress masks the true active stress, and that restoring stress functions as an effective "brake" for active shortening below the slack SL.
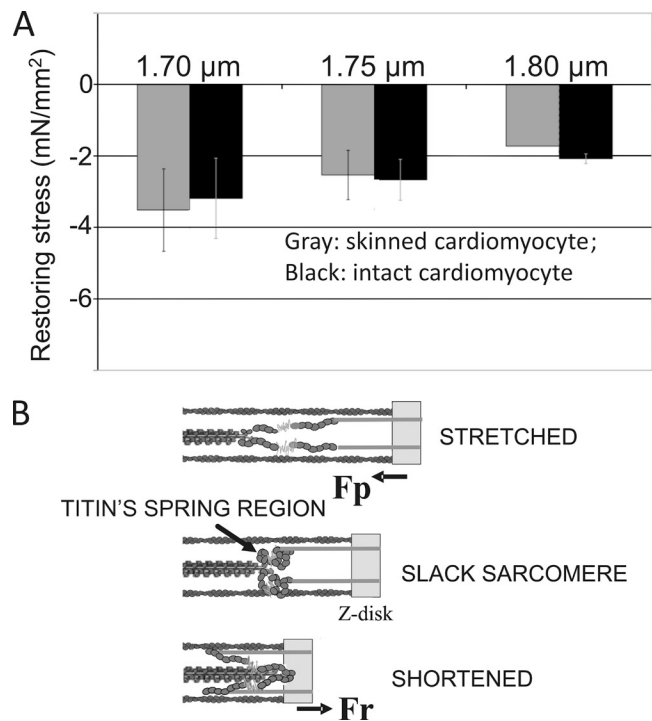


**Figure 7.** Comparison of restoring stress of intact and skinned cardiac myocytes and model of titin-based restoring stress development. (A) Intact myocytes (this study) and skinned myocytes (Helmes et al., 1996) at the three shown SLs (1.7, 1.75, and 1.8 µm). Restoring stresses in the two different types of preparations are similar. (B) Schematic of titin's spring region in a sarcomere that is slack (middle), stretched to above slack (top), or shortened to below slack (bottom). The spring region is flaccid in slack sarcomeres and is held away from the Z-disk by the inextensible near–Z-disk region of titin (gray). When the sarcomere is stretched above the slack SL, titin's spring region is stretched in a direction that results in a passive force (Fp) that tends to shorten the sarcomere. When the sarcomere shortens to below slack, the thick filament tip moves into the stiff near–Z-disk region, and titin's spring region is stretched in a direction that results in a restoring force (Fr) that pushes outward on the Z-disk.

To gain insights into whether restoring stress levels of intact cells are different from those of skinned cells, we compared our results to the previous work of Helmes et al. (1996) that used rigor contraction of skinned cells that were first buckled below slack and that upon relaxation remained below slack and developed restoring stress. Results of skinned and intact cells are indistinguishable (Fig. 7 A). This suggests that cytosolic proteins, the plasma membrane, and microtubules do not significantly contribute to restoring stress. Our findings were also compared with a study on intact rat trabeculae in which restoring stress was determined via a rapid cooling contraction (top part of Fig. 4.5 in Backx, 1989). The mean restoring stress values of the trabeculae were $-5.1$, $-3.5$, and $-2.0$ mN/mm$^2$ at the SL ranges shown in Fig. 7 (from short to long), suggesting that the majority of restoring stress of trabeculae is attributable to a cell-based mechanism with a smaller involvement from the extracellular matrix.

Titin-based restoring stress will only contribute to the suction that underlies early diastolic left ventricular filling if the end-systolic SL will be below the slack SL ($\sim$1.95 µm). There is a relative paucity of in vivo SL data, with most estimates of the in vivo SL in the arrested zero pressure rodent heart at or slightly below 2.0 µm (for details and original citations, see Bub et al., 2010) and in the arrested LV of larger mammals at or slightly above 2.0 µm (for details and original citations, see LeWinter et al., 2010). The minimum systolic SL will be below these SL values measured in the arrested heart; therefore, it seems possible that titin-based restoring stress will contribute to diastolic suction. Additional work is needed to more firmly establish the end-systolic SL under physiological and pathological conditions, including diastolic dysfunction and heart failure.

## Summary

The diastolic properties of intact and skinned mouse cardiac myocyte were studied. At physiological temperatures, intact cells generate actomyosin-based active stress; when actomyosin interaction is inhibited, the passive and restoring stresses of intact and skinned cells are similar. Comparison with previous results indicates that the majority of restoring stress of muscle is attributable to a cell-based mechanism. Findings of this work contribute to the understanding of diastolic function and are relevant for future studies of the mechanisms that underlie the elevated diastolic stress of DHF patients.

Richard L. Moss served as editor.

### REFERENCES

Adhikari, B.B., M. Regnier, A.J. Rivera, K.L. Kreutziger, and D.A. Martyn. 2004. Cardiac length dependence of force and force redevelopment kinetics with altered cross-bridge cycling. *Biophys. J.* 87:1784–1794. doi:10.1529/biophysj.103.039131

Backx, P.H. 1989. The force-sarcomere length relationship in rat cardiac muscle. PhD thesis. University of Calgary, Calgary, Canada. 116 pp.

Backx, P.H., W.D. Gao, M.D. Azan-Backx, and E. Marban. 1994. Mechanism of force inhibition by 2,3-butanedione monoxime in rat cardiac muscle: roles of [Ca2+]i and cross-bridge kinetics. *J. Physiol.* 476:487–500.

Bell, S.P., J. Fabian, and M.M. LeWinter. 1998. Effects of dobutamine on left ventricular restoring forces. *Am. J. Physiol.* 275:H190–H194.

Bluhm, W.F., A.D. McCulloch, and W.Y. Lew. 1995. Active force in rabbit ventricular myocytes. *J. Biomech.* 28:1119–1122. doi:10.1016/0021-9290(94)00018-Y

Borbély, A., J. van der Velden, Z. Papp, J.G. Bronzwaer, I. Edes, G.J. Stienen, and W.J. Paulus. 2005. Cardiomyocyte stiffness in diastolic heart failure. *Circulation.* 111:774–781. doi:10.1161/01.CIR.0000155257.33485.6D

Borbély, A., I. Falcao-Pires, L. van Heerebeek, N. Hamdani, I. Edes, C. Gavina, A.F. Leite-Moreira, J.G. Bronzwaer, Z. Papp, J. van der Velden, et al. 2009a. Hypophosphorylation of the stiff N2B titin isoform raises cardiomyocyte resting tension in failing human myocardium. *Circ. Res.* 104:780–786. doi:10.1161/CIRCRESAHA.108.193326

Borbély, A., L. van Heerebeek, and W.J. Paulus. 2009b. Transcriptional and posttranslational modifications of titin: implications for diastole. *Circ. Res.* 104:12–14. doi:10.1161/CIRCRESAHA.108.191130

Brady, A.J. 1991. Mechanical properties of isolated cardiac myocytes. *Physiol. Rev.* 71:413–428.

Bronzwaer, J.G., and W.J. Paulus. 2005. Matrix, cytoskeleton, or myofilaments: which one to blame for diastolic left ventricular dysfunction? *Prog. Cardiovasc. Dis.* 47:276–284. doi:10.1016/j.pcad.2005.02.003

Bub, G., P. Camelliti, C. Bollensdorff, D.J. Stuckey, G. Picton, R.A. Burton, K. Clarke, and P. Kohl. 2010. Measurement and analysis of sarcomere length in rat cardiomyocytes in situ and in vitro. *Am. J. Physiol. Heart Circ. Physiol.* 298:H1616–H1625. doi:10.1152/ajpheart.00481.2009

Fabiato, A., and F. Fabiato. 1979. Calculator programs for computing the composition of the solutions containing multiple metals and ligands used for experiments in skinned muscle cells. *J. Physiol. (Paris).* 75:463–505.

Farman, G.P., J.S. Walker, P.P. de Tombe, and T.C. Irving. 2006. Impact of osmotic compression on sarcomere structure and myofilament calcium sensitivity of isolated rat myocardium. *Am. J. Physiol. Heart Circ. Physiol.* 291:H1847–H1855. doi:10.1152/ajpheart.01237.2005

Farman, G.P., K. Tachampa, R. Mateja, O. Cazorla, A. Lacampagne, and P.P. de Tombe. 2008. Blebbistatin: use as inhibitor of muscle contraction. *Pflugers Arch.* 455:995–1005. doi:10.1007/s00424-007-0375-3

Flagg, T.P., O. Cazorla, M.S. Remedi, T.E. Haim, M.A. Tones, A. Bahinski, R.E. Numann, A. Kovacs, J.E. Schaffer, C.G. Nichols, and J.M. Nerbonne. 2009. Ca2+-independent alterations in diastolic sarcomere length and relaxation kinetics in a mouse model of lipotoxic diabetic cardiomyopathy. *Circ. Res.* 104:95–103. doi:10.1161/CIRCRESAHA.108.186809

Gao, W.D., P.H. Backx, M. Azan-Backx, and E. Marban. 1994. Myofilament Ca2+ sensitivity in intact versus skinned rat ventricular muscle. *Circ. Res.* 74:408–415.

Gao, W.D., N.G. Perez, and E. Marban. 1998. Calcium cycling and contractile activation in intact mouse cardiac muscle. *J. Physiol.* 507:175–184. doi:10.1111/j.1469-7793.1998.175bu.x

Granzier, H.L., and T.C. Irving. 1995. Passive tension in cardiac muscle: contribution of collagen, titin, microtubules, and intermediate filaments. *Biophys. J.* 68:1027–1044. doi:10.1016/S0006-3495(95)80278-X

Granzier, H., M. Helmes, O. Cazorla, M. McNabb, D. Labeit, Y. Wu, R. Yamasaki, A. Redkar, M. Kellermayer, S. Labeit, and K. Trombitas. 2000. Mechanical properties of titin isoforms. *Adv. Exp. Med. Biol.* 481:283–300.

Hamdani, N., M. de Waard, A.E. Messer, N.M. Boontje, V. Kooij, S. van Dijk, A. Versteilen, R. Lamberts, D. Merkus, C. Dos Remedios, et al. 2008. Myofilament dysfunction in cardiac disease from mice to men. *J. Muscle Res. Cell Motil.* 29:189–201. doi:10.1007/s10974-008-9160-y

Harrison, S.M., and D.M. Bers. 1989. Influence of temperature on the calcium sensitivity of the myofilaments of skinned ventricular muscle from the rabbit. *J. Gen. Physiol.* 93:411–428.

Harrison, S.M., and D.M. Bers. 1990. Temperature dependence of myofilament Ca sensitivity of rat, guinea pig, and frog ventricular muscle. *Am. J. Physiol.* 258:C274–C281.

Helmes, M., K. Trombitás, and H. Granzier. 1996. Titin develops restoring force in rat cardiac myocytes. *Circ. Res.* 79:619–626.

Helmes, M., C.C. Lim, R. Liao, A. Bharti, L. Cui, and D.B. Sawyer. 2003. Titin determines the Frank-Starling relation in early diastole. *J. Gen. Physiol.* 121:97–110. doi:10.1085/jgp.20028652

Herrmann, C., J. Wray, F. Travers, and T. Barman. 1992. Effect of 2,3-butanedione monoxime on myosin and myofibrillar ATPases. An example of an uncompetitive inhibitor. *Biochemistry.* 31:12227–12232. doi:10.1021/bi00163a036

Iribe, G., M. Helmes, and P. Kohl. 2007. Force-length relations in isolated intact cardiomyocytes subjected to dynamic changes in mechanical load. *Am. J. Physiol. Heart Circ. Physiol.* 292:H1487–H1497. doi:10.1152/ajpheart.00909.2006

Irving, T.C., J. Konhilas, D. Perry, R. Fischetti, and P.P. de Tombe. 2000. Myofilament lattice spacing as a function of sarcomere length in isolated rat myocardium. *Am. J. Physiol. Heart Circ. Physiol.* 279:H2568–H2573.

Kass, D.A., J.G. Bronzwaer, and W.J. Paulus. 2004. What mechanisms underlie diastolic dysfunction in heart failure? *Circ. Res.* 94:1533–1542. doi:10.1161/01.RES.0000129254.25507.d6

Kentish, J.C., H.E. ter Keurs, L. Ricciardi, J.J. Bucx, and M.I. Noble. 1986. Comparison between the sarcomere length-force relations of intact and skinned trabeculae from rat right ventricle. Influence of calcium concentrations on these relations. *Circ. Res.* 58:755–768.

Kovács, M., J. Tóth, C. Hetényi, A. Málnási-Csizmadia, and J.R. Sellers. 2004. Mechanism of blebbistatin inhibition of myosin II. *J. Biol. Chem.* 279:35557–35563. doi:10.1074/jbc.M405319200

Krüger, M., and W.A. Linke. 2009. Titin-based mechanical signalling in normal and failing myocardium. *J. Mol. Cell. Cardiol.* 46:490–498. doi:10.1016/j.yjmcc.2009.01.004

Labeit, S., and B. Kolmerer. 1995. Titins: giant proteins in charge of muscle ultrastructure and elasticity. *Science.* 270:293–296. doi:10.1126/science.270.5234.293

Lahmers, S., Y. Wu, D.R. Call, S. Labeit, and H. Granzier. 2004. Developmental control of titin isoform expression and passive stiffness in fetal and neonatal myocardium. *Circ. Res.* 94:505–513. doi:10.1161/01.RES.0000115522.52554.86

Le Guennec, J.Y., N. Peineau, J.A. Argibay, K.G. Mongo, and D. Garnier. 1990. A new method of attachment of isolated mammalian ventricular myocytes for tension recording: length dependence of passive and active tension. *J. Mol. Cell. Cardiol.* 22:1083–1093. doi:10.1016/0022-2828(90)90072-A

LeWinter, M.M., and H. Granzier. 2010. Cardiac titin: a multifunctional giant. *Circulation.* 121:2137–2145. doi:10.1161/CIRCULATIONAHA.109.860171

LeWinter, M.M., J. Popper, M. McNabb, L. Nyland, S.B. Bell, and H. Granzier. 2010. Extensible behavior of titin in the miniswine left ventricle. *Circulation.* 121:768–774. doi:10.1161/CIRCULATIONAHA.109.918151

Lorenzen-Schmidt, I., B.D. Stuyvers, H.E. ter Keurs, M.O. Date, M. Hoshijima, K.R. Chien, A.D. McCulloch, and J.H. Omens. 2005. Young MLP deficient mice show diastolic dysfunction before the onset of dilated cardiomyopathy. *J. Mol. Cell. Cardiol.* 39:241–250. doi:10.1016/j.yjmcc.2005.05.006

Nash, G.B., P.E. Tatham, T. Powell, V.W. Twist, R.D. Speller, and L.T. Loverock. 1979. Size measurements on isolated rat heart cells using Coulter analysis and light scatter flow cytometry. *Biochim. Biophys. Acta.* 587:99–111.

Neagoe, C., C.A. Opitz, I. Makarenko, and W.A. Linke. 2003. Gigantic variety: expression patterns of titin isoforms in striated muscles and consequences for myofibrillar passive stiffness. *J. Muscle Res. Cell Motil.* 24:175–189. doi:10.1023/A:1026053530766

Niggli, E. 1988. A laser diffraction system with improved sensitivity for long-time measurements of sarcomere dynamics in isolated cardiac myocytes. *Pflugers Arch.* 411:462–468. doi:10.1007/BF00587728

Nishimura, R.A., and W. Jaber. 2007. Understanding "diastolic heart failure": the tip of the iceberg. *J. Am. Coll. Cardiol.* 49:695–697. doi:10.1016/j.jacc.2006.11.014

O'Connell, T.D., M.C. Rodrigo, and P.C. Simpson. 2007. Isolation and culture of adult mouse cardiac myocytes. *Methods Mol. Biol.* 357:271–296.

Owan, T.E., D.O. Hodge, R.M. Herges, S.J. Jacobsen, V.L. Roger, and M.M. Redfield. 2006. Trends in prevalence and outcome of heart failure with preserved ejection fraction. *N. Engl. J. Med.* 355:251–259. doi:10.1056/NEJMoa052256

Preetha, N., W. Yiming, M. Helmes, F. Norio, L. Siegfried, and H. Granzier. 2005. Restoring force development by titin/connectin and assessment of Ig domain unfolding. *J. Muscle Res. Cell Motil.* 26:307–317. doi:10.1007/s10974-005-9037-2

Roos, K.P., and A.J. Brady. 1989. Stiffness and shortening changes in myofilament-extracted rat cardiac myocytes. *Am. J. Physiol.* 256:H539–H551.

Stuyvers, B.D., M. Miura, and H.E. ter Keurs. 1997. Dynamics of viscoelastic properties of rat cardiac sarcomeres during the diastolic interval: involvement of Ca2+. *J. Physiol.* 502:661–677. doi:10.1111/j.1469-7793.1997.661bj.x

Stuyvers, B.D., A.D. McCulloch, J. Guo, H.J. Duff, and H.E. ter Keurs. 2002. Effect of stimulation rate, sarcomere length and Ca(2+) on force generation by mouse cardiac muscle. *J. Physiol.* 544:817–830. doi:10.1113/jphysiol.2002.024430

Ter Keurs, H.E., T. Shinozaki, Y.M. Zhang, Y. Wakayama, Y. Sugai, Y. Kagaya, M. Miura, P.A. Boyden, B.D. Stuyvers, and A. Landesberg. 2008. Sarcomere mechanics in uniform and nonuniform cardiac muscle: a link between pump function and arrhythmias. *Ann. NY Acad. Sci.* 1123:79–95. doi:10.1196/annals.1420.010

Trombitás, K., and H. Granzier. 1997. Actin removal from cardiac myocytes shows that near Z line titin attaches to actin while under tension. *Am. J. Physiol.* 273:C662–C670.

Trombitás, K., A. Freiburg, M. Greaser, S. Labeit, and H. Granzier. 2000. From connecting filaments to co-expression of titin isoforms. *Adv. Exp. Med. Biol.* 481:405–418.

Trombitás, K., Y. Wu, D. Labeit, S. Labeit, and H. Granzier. 2001. Cardiac titin isoforms are coexpressed in the half-sarcomere and extend independently. *Am. J. Physiol. Heart Circ. Physiol.* 281:H1793–H1799.

Warren, C.M., P.R. Krzesinski, and M.L. Greaser. 2003. Vertical agarose gel electrophoresis and electroblotting of high-molecular-weight proteins. *Electrophoresis.* 24:1695–1702. doi:10.1002/elps.200305392

Wussling, M., W. Schenk, and B. Nilius. 1987. A study of dynamic properties in isolated myocardial cells by the laser diffraction method. *J. Mol. Cell. Cardiol.* 19:897–907. doi:10.1016/S0022-2828(87)80618-1

Yasuda, S.I., S. Sugiura, N. Kobayakawa, H. Fujita, H. Yamashita, K. Katoh, Y. Saeki, H. Kaneko, Y. Suda, R. Nagai, and H. Sugi. 2001. A novel method to study contraction characteristics of a single cardiac myocyte using carbon fibers. *Am. J. Physiol. Heart Circ. Physiol.* 281:H1442–H1446.

Yasuda, S., D. Townsend, D.E. Michele, E.G. Favre, S.M. Day, and J.M. Metzger. 2005. Dystrophic heart failure blocked by membrane sealant poloxamer. *Nature.* 436:1025–1029. doi:10.1038/nature03844

Zile, M.R., and D.L. Brutsaert. 2002a. New concepts in diastolic dysfunction and diastolic heart failure: part I: diagnosis, prognosis, and measurements of diastolic function. *Circulation.* 105:1387–1393. doi:10.1161/hc1102.105289

Zile, M.R., and D.L. Brutsaert. 2002b. New concepts in diastolic dysfunction and diastolic heart failure: part II: causal mechanisms and treatment. *Circulation.* 105:1503–1508. doi:10.1161/hc1202.105290